J. Plasma Phys. (2022), *vol.* 88, 905880319
Published by Cambridge University Press

doi:10.1017/S0022377822000514

A generalized Hasegawa–Mima equation in curved magnetic fields

Naoki Sato[1,†] **and Michio Yamada**[2]

[1]Graduate School of Frontier Sciences, The University of Tokyo, Kashiwa, Chiba 277-8561, Japan

[2]Research Institute for Mathematical Sciences, Kyoto University, Kyoto 606-8502, Japan

(Received 11 December 2021; revised 19 May 2022; accepted 20 May 2022)

We derive a model equation describing electrostatic plasma turbulence in general (inhomogeneous and curved) magnetic fields by analysing the effect of curved geometry on the ion fluid polarization drift velocity. The derived nonlinear equation generalizes the Hasegawa–Mima equation governing drift wave turbulence in a straight homogeneous magnetic field, and may serve as a toy model for the description of turbulent plasmas. The equation is most appropriate for configurations with a small $\boldsymbol{E}\times\boldsymbol{B}$ drift velocity divergence, or a mild spatial change in $\boldsymbol{E}\times\boldsymbol{B}$ drift velocity. We identify the conserved energy of the system, and obtain conditions on magnetic field topology for conservation of generalized enstrophy. Through numerical examples, we further show how the curvature of the magnetic field reshapes self-organized steady turbulent states.

Key word: plasma nonlinear phenomena

1. Introduction

The Hasegawa–Mima equation (Hasegawa & Mima 1977*a*,*b*) describes two-dimensional electrostatic plasma turbulence in a straight homogeneous magnetic field. Mathematically, it is related to the quasi-geostrophic equation for atmospheric dynamics on rotating planetary surfaces (Charney 1948; Charney & Drazin 1961), and it reduces to the vorticity equation for a two-dimensional incompressible fluid in the limit of high electron temperature (Horton & Hasegawa 1994). As such, the Hasegawa–Mima equation exhibits properties analogous to two-dimensional fluid turbulence (Batchelor 1969; Kraichnan & Montgomery 1980; Dritschel, Qi & Marston 2015), including inverse cascade of energy (Kraichnan 1967; Rivera *et al.* 2003; Xiao *et al.* 2009) associated with the presence of two inviscid invariants, energy and generalized enstrophy (Hasegawa & Mima 2018). Furthermore, in the inviscid limit the system is endowed with a non-canonical Hamiltonian structure (Weinstein 1983; Morrison 1998), where energy and generalized enstrophy play the roles of Hamiltonian and Casimir invariant, respectively (Tassi, Chandre & Morrison 2009). These properties combined with a relative simplicity make the Hasegawa–Mima equation an effective tool in the study of two-dimensional fluid and plasma turbulence.

† Email address for correspondence: sato_naoki@edu.k.u-tokyo.ac.jp

Applications include the investigation of turbulence in geophysical flows (Nazarenko & Quinn 2009) and magnetically confined plasmas (Horton 1999; Fujisawa *et al.* 2004), and more generally the characterization of self-organized turbulent states and zonal flows (Diamond, Hasegawa & Mima 2011; Singh & Diamond 2021).

Several generalizations of the Hasegawa–Mima equation exist. On the one hand, the Hasegawa–Wakatani system (Hasegawa & Wakatani 1983; Wakatani & Hasegawa 1984) consists of coupled nonlinear equations for the electrostatic potential and the ion density. These equations reveal the interplay between drift wave turbulence and zonal flow mediated by the Kelvin–Helmholtz instability (Numata, Ball & Dewar 2007). Hasegawa and Wakatani also included the effect of field curvature in cylindrical geometry in their equations (Hasegawa & Wakatani 1987). On the other hand, reduced magnetohydrodynamics (Hazeltine 1983) and the four-field model (Hazeltine, Hsu & Morrison 1987) take into account the time evolution of magnetic flux, parallel ion velocity and electron pressure. Nevertheless, these models are two-dimensional, any deviation from a straight magnetic field being treated as a higher-order correction in the relevant ordering. Hence, a closed equation for the electric potential describing electrostatic plasma turbulence in a general magnetic field is not available at present. This deficiency, which can be ascribed to the rather elusive nature of the polarization drift (Cary & Brizard 2009; Kaufman 1986) in non-trivial magnetic fields, has made the understanding of the impact of topology on the evolution of turbulence a difficult task because one usually needs to resort to complete models, such as gyrokinetic theory. In this context, the development of a pertinent toy equation may allow a simplified modelling of turbulence in complex plasma systems, and therefore help to elucidate the nonlinear physics of two-dimensional turbulence in non-uniform magnetic fields. Indeed, the Hasegawa–Mima equation and similar two-dimensional fluid equations have been useful in studying long-term evolution of coherent structures in Rossby wave turbulence including zonal flows (Yoden & Yamada 1993; Obuse, Takehiro & Yamada 2010).

The purpose of this paper is to fill such theoretical gap by deriving an equation describing the evolution of electrostatic turbulence in a general magnetic field for the simplest plasma system consisting of cold ions and a cloud of electrons obeying the Boltzmann distribution. As in the classical construction, in principle two approaches could be followed to obtain such an equation: gyrokinetic theory or a fluid description. In the former, one proceeds by integration of the guiding centre distribution function to obtain an equation for ion density fluctuations that leads to Hasegawa–Mima-type electrostatic turbulence by coupling with the gyrokinetic Poisson equation upon suitable assumptions including cold ions and an adiabatic electron response (Dubin, Krommes & Oberman 1983; Krommes 2002). It should be noted that, in this context, turbulence is mediated by a polarization density (Brizard & Hahm 2007) rather than a polarization drift velocity. By contrast, in the fluid approach one starts from the ion continuity equation and substitutes the relevant ion $\boldsymbol{E} \times \boldsymbol{B}$ and polarization drift velocities (which are fluid and not guiding centre velocities) obtained from ion fluid momentum balance, and derives a closed equation for the electrostatic potential (see e.g. Hazeltine & Waelbroeck (1998) on the treatment of drift motion within the fluid formalism). In this paper we follow the fluid formalism, sticking to the original derivation carried out by Hasegawa and Mima (Hasegawa & Mima 1977*a*), although we expect an equivalent construction to be possible within the gyrokinetic framework as well.

2. Electrostatic potential in curved magnetic fields

Consider a plasma system consisting of ions and electrons. Let n_e denote the electron density. We assume that n_e follows a Boltzmann distribution with constant

https://doi.org/10.1017/S0022377822000514 Published online by Cambridge University Press

temperature $T_e > 0$:

$$n_e = A_e \exp\left\{-\frac{q\phi}{k_B T_e}\right\}. \tag{2.1}$$

Here, $A_e(\boldsymbol{x})$ is a positive spatial function, ϕ denotes the electric potential, $q = -e$ is the electron charge and k_B is the Boltzmann constant. It is convenient to introduce the constant

$$\lambda = \frac{e}{k_B T_e}. \tag{2.2}$$

Let $\boldsymbol{B} = \boldsymbol{B}(\boldsymbol{x})$ denote a static magnetic field. Recall that $\boldsymbol{B}$ must be solenoidal, $\nabla \cdot \boldsymbol{B} = 0$. In the following, we demand that $\boldsymbol{B} \neq 0$ throughout the domain of interest V. Let n denote the ion density. Assuming quasi-neutrality, $n_e = Zn$ with Z the number of protons in the ions. Using (2.1), the ion continuity equation reads

$$\lambda\phi_t = -\nabla \cdot \boldsymbol{v} - \lambda \boldsymbol{v} \cdot \nabla\phi - \nabla \log A_e \cdot \boldsymbol{v}. \tag{2.3}$$

Here, $\boldsymbol{v}$ denotes the ion fluid velocity. On the other hand, denoting with m the ion mass, the ion fluid equation of motion can be written as

$$mn\frac{\mathrm{d}\boldsymbol{v}}{\mathrm{d}t} = Zen\left(\boldsymbol{v} \times \boldsymbol{B} + \boldsymbol{E}\right) - \nabla P, \tag{2.4}$$

where P represents pressure and $\boldsymbol{E} = -\nabla\phi$ the electric field. It is convenient to decompose the ion fluid velocity as

$$\boldsymbol{v} = \boldsymbol{v}_{\parallel} + \boldsymbol{v}_{\perp}, \tag{2.5}$$

where $\boldsymbol{v}_{\parallel}$ denotes the velocity component along the magnetic field and $\boldsymbol{v}_{\perp}$ the perpendicular one. In the two-dimensional drift turbulence setting, the parallel velocity component is neglected because the time scale of fluctuations t_d is faster than the time scale t_b of ion dynamics along the magnetic field, $t_d \ll t_b$. In the following, we will therefore put

$$\boldsymbol{v}_{\parallel} = \boldsymbol{0}, \tag{2.6}$$

and discard the dynamics along $\boldsymbol{B}$. In this context, it is of interest to study the long-term evolution of coherent structures. It is worth noticing that in the opposite regime $t_d \gg t_b$ the parallel motion $\boldsymbol{v}_{\parallel}$ gets averaged out as well due to the fast bounce oscillation, although the polarization drift becomes neoclassically enhanced due to a large orbit size, leading to a neoclassically modified turbulence model with a dominant Hasegawa–Mima-type polarization nonlinearity (Hahm & Tang 1996). To proceed, we introduce a reference time scale t_c and a reference length scale $L_{\perp}$ across $\boldsymbol{B}$, and take $k_B T_e$ as reference value for the energy. In the standard drift turbulence ordering $t_c = 2\pi/\Omega_c$, with $\Omega_c = ZeB/m$ the ion cyclotron frequency, while $L_{\perp}$ corresponds to the sound radius $\rho_s = c_s\Omega_c^{-1} \sim k_{\perp}^{-1}$, where $c_s = (Zk_B T_e/m)^{1/2}$ is the sound speed and $k_{\perp}$ a characteristic perpendicular wavenumber for the turbulence. In this study we further consider a regime of plasma where the electric potential energy is small compared with the electron kinetic energy, and the ratio between the component of the electric field perpendicular to the magnetic field and the magnetic field itself is small:

$$\left|\frac{e\phi}{k_B T_e}\right| \sim \epsilon, \quad \frac{t_c E_{\perp}}{L_{\perp} B} \sim \epsilon, \tag{2.7a,b}$$

where $\epsilon \ll 1$ is a small ordering parameter, $E_{\perp} = |\boldsymbol{E}_{\perp}|$, with $\boldsymbol{E}_{\perp}$ the component of the electric field $\boldsymbol{E}$ perpendicular to $\boldsymbol{B}$, and $B = |\boldsymbol{B}|$. The remaining perpendicular component

https://doi.org/10.1017/S0022377822000514 Published online by Cambridge University Press

$\boldsymbol{v}_\perp$ can be expanded into a first-order term $\boldsymbol{v}_1$, which will correspond to first-order $\boldsymbol{E}\times\boldsymbol{B}$ drift dynamics, a second-order term $\boldsymbol{v}_2$, which will be identified with second-order $\boldsymbol{E}\times\boldsymbol{B}$ drift dynamics plus the polarization drift encountered in guiding centre theory, and higher-order corrections. At second order in ϵ we therefore have

$$\boldsymbol{v} = \boldsymbol{v}_\perp = \epsilon\boldsymbol{v}_1 + \epsilon^2\boldsymbol{v}_2. \tag{2.8}$$

To proceed, a further working assumption is needed on the rate of change of $\boldsymbol{v}$, which may only evolve on time scales long relative to a gyroperiod:

$$\frac{t_c}{|\boldsymbol{v}|}\frac{\partial\boldsymbol{v}}{\partial t} \ll 1. \tag{2.9}$$

Recalling the decomposition (2.8), (2.9) leads to

$$\frac{t_c^2}{L_\perp}\left|\frac{\partial\boldsymbol{v}_1}{\partial t}\right| \sim \epsilon, \quad \frac{t_c^2}{L_\perp}\left|\frac{\partial\boldsymbol{v}_2}{\partial t}\right| \sim \epsilon. \tag{2.10a,b}$$

Furthermore, we enforce the cold ion hypothesis $T = 0$, with T the ion temperature, implying that ions are not subject to thermal fluctuations, and therefore

$$P = 0. \tag{2.11}$$

To obtain expressions for $\boldsymbol{v}_1$ and $\boldsymbol{v}_2$, consider again the equation of motion (2.4), which at second order in ϵ now reads as

$$\epsilon Ze\left(\boldsymbol{B}\times\boldsymbol{v}_1 - \boldsymbol{E}_1\right) = \epsilon^2\left[-m\frac{\mathrm{d}\boldsymbol{v}_1}{\mathrm{d}t} + Ze\left(\boldsymbol{v}_2\times\boldsymbol{B} + \boldsymbol{E}_2\right)\right]. \tag{2.12}$$

Here, we used (2.10*a*,*b*) to extract the order of $\partial\boldsymbol{v}_1/\partial t$ according to $\partial\boldsymbol{v}_1/\partial t \to \epsilon\partial\boldsymbol{v}_1/\partial t$. In addition, the electric potential ϕ and electric field $\boldsymbol{E}$ have been decomposed into first-order and second-order components according to

$$\phi = \epsilon\phi_1 + \epsilon^2\phi_2, \quad \boldsymbol{E} = \epsilon\boldsymbol{E}_1 + \epsilon^2\boldsymbol{E}_2 = -\epsilon\nabla\phi_1 - \epsilon^2\nabla\phi_2. \tag{2.13a,b}$$

Hence, the cross product of (2.12) with $\boldsymbol{B}/B^2$ can be cast in the form

$$\epsilon\left(\frac{\boldsymbol{E}_1\times\boldsymbol{B}}{B^2} - \boldsymbol{v}_1\right) = \epsilon^2\left[-\sigma\frac{\boldsymbol{B}\times\dfrac{\mathrm{d}\boldsymbol{v}_1}{\mathrm{d}t}}{B^2} + \boldsymbol{v}_2 + \frac{\boldsymbol{B}\times\boldsymbol{E}_2}{B^2}\right], \tag{2.14}$$

where we introduced the physical constant

$$\sigma = \frac{m}{Ze}. \tag{2.15}$$

Notice that all terms on the left-hand side of (2.14) are first order in ϵ, while those on the right-hand side are second order. The first-order $\boldsymbol{E}\times\boldsymbol{B}$ flow $\boldsymbol{v}_{E_1}$ can be obtained from the

https://doi.org/10.1017/S0022377822000514 Published online by Cambridge University Press

left-hand side:

$$\boldsymbol{v}_1 = \boldsymbol{v}_{E_1} = \frac{\boldsymbol{E}_1 \times \boldsymbol{B}}{B^2}. \tag{2.16}$$

Similarly, the second-order fluid drift is given by

$$\boldsymbol{v}_2 = \boldsymbol{v}_{\text{pol}} + \boldsymbol{v}_{E_2} = \sigma \frac{\boldsymbol{B} \times \dfrac{\mathrm{d}\boldsymbol{v}_1}{\mathrm{d}t}}{B^2} + \frac{\boldsymbol{E}_2 \times \boldsymbol{B}}{B^2}. \tag{2.17}$$

Evidently, the second term on the right-hand side is a second-order $\boldsymbol{E} \times \boldsymbol{B}$ drift $\boldsymbol{v}_{E_2}$, while the first term is nothing but a polarization drift $\boldsymbol{v}_{\text{pol}}$ (see Hazeltine & Waelbroeck 1998). Indeed, in a straight magnetic field $\boldsymbol{B} = B_0 \nabla z$ with $B_0 \in \mathbb{R}$ one has

$$\boldsymbol{v}_{\text{pol}} = \sigma \frac{\boldsymbol{B} \times \dfrac{\mathrm{d}\boldsymbol{v}_1}{\mathrm{d}t}}{B^2} = \frac{\sigma}{B_0^2} \frac{\mathrm{d}\boldsymbol{E}_{1\perp}}{\mathrm{d}t}, \tag{2.18}$$

with $\boldsymbol{E}_{1\perp}$ the component of $\boldsymbol{E}_1$ perpendicular to $\boldsymbol{B}$. Combining equations (2.16) and (2.17), the total ion velocity has the expression

$$\begin{aligned} \boldsymbol{v} &= \epsilon \boldsymbol{v}_{E_1} - \epsilon^2 \sigma \frac{\boldsymbol{B} \times \left[\boldsymbol{v}_{E_1} \times \left(\nabla \times \boldsymbol{v}_{E_1}\right)\right]}{B^2} - \epsilon^2 \sigma \frac{\partial}{\partial t} \frac{\nabla_\perp \phi_1}{B^2} + \epsilon^2 \sigma \frac{\boldsymbol{B} \times \nabla \left(\boldsymbol{v}_{E_1}^2 + \phi_2\right)}{2B^2} \\ &= \epsilon \left(1 - \epsilon \sigma \frac{\boldsymbol{B} \boldsymbol{\cdot} \nabla \times \boldsymbol{v}_{E_1}}{B^2}\right) \boldsymbol{v}_{E_1} - \epsilon^2 \sigma \frac{\partial}{\partial t} \frac{\nabla_\perp \phi_1}{B^2} + \epsilon^2 \sigma \frac{\boldsymbol{B} \times \nabla \left(\boldsymbol{v}_{E_1}^2 + \phi_2\right)}{2B^2}, \end{aligned} \tag{2.19}$$

where we introduced the orthogonal gradient operator

$$\nabla_\perp f = \frac{\boldsymbol{B} \times (\nabla f \times \boldsymbol{B})}{B^2}, \tag{2.20}$$

with f some function. Then, we have

$$\begin{aligned} \nabla \boldsymbol{\cdot} \boldsymbol{v} = \nabla \boldsymbol{\cdot} \left[\epsilon \left(1 - \epsilon \sigma \frac{\boldsymbol{B} \boldsymbol{\cdot} \nabla \times \boldsymbol{v}_{E_1}}{B^2}\right) \boldsymbol{v}_{E_1}\right] - \epsilon^2 \sigma \frac{\partial}{\partial t} \nabla \boldsymbol{\cdot} \left(\frac{\nabla_\perp \phi_1}{B^2}\right) \\ + \frac{1}{2} \epsilon^2 \sigma \nabla \left(\boldsymbol{v}_{E_1}^2 + \phi_2\right) \boldsymbol{\cdot} \nabla \times \left(\frac{\boldsymbol{B}}{B^2}\right). \end{aligned} \tag{2.21}$$

Defining the total $\boldsymbol{E} \times \boldsymbol{B}$ drift velocity as

$$\boldsymbol{v}_E = \epsilon \boldsymbol{v}_{E_1} + \epsilon^2 \boldsymbol{v}_{E_2} = \frac{\boldsymbol{E} \times \boldsymbol{B}}{B^2}, \tag{2.22}$$

at second order equation (2.19) can be expressed solely in terms of ϕ as

$$\begin{aligned} \boldsymbol{v} &= \boldsymbol{v}_E - \sigma \frac{\boldsymbol{B} \times [\boldsymbol{v}_E \times (\nabla \times \boldsymbol{v}_E)]}{B^2} - \sigma \frac{\partial}{\partial t} \frac{\nabla_\perp \phi}{B^2} + \sigma \frac{\boldsymbol{B} \times \nabla \boldsymbol{v}_E^2}{2B^2} \\ &= \left(1 - \sigma \frac{\boldsymbol{B} \boldsymbol{\cdot} \nabla \times \boldsymbol{v}_E}{B^2}\right) \boldsymbol{v}_E - \sigma \frac{\partial}{\partial t} \frac{\nabla_\perp \phi}{B^2} + \sigma \frac{\boldsymbol{B} \times \nabla \boldsymbol{v}_E^2}{2B^2}. \end{aligned} \tag{2.23}$$

We remark that this same result can also be obtained by a simple iteration method where, regarding the left-hand side of (2.4) as a smaller term than the right-hand side, we have the

https://doi.org/10.1017/S0022377822000514 Published online by Cambridge University Press

lowest-order solution as $\boldsymbol{v} = \boldsymbol{v}_E$ and the next-order solution as given by (2.23). Similarly, in terms of ϕ, (2.21) can be written as

$$\nabla\cdot\boldsymbol{v} = \nabla\cdot\left[\left(1-\sigma\frac{\boldsymbol{B}\cdot\nabla\times\boldsymbol{v}_E}{B^2}\right)\boldsymbol{v}_E\right] - \sigma\frac{\partial}{\partial t}\nabla\cdot\left(\frac{\nabla_\perp\phi}{B^2}\right) + \frac{1}{2}\sigma\nabla\boldsymbol{v}_E^2\cdot\nabla\times\left(\frac{\boldsymbol{B}}{B^2}\right). \tag{2.24}$$

On the other hand, the term

$$\lambda\boldsymbol{v}\cdot\nabla\phi = \epsilon^3\lambda\left(\boldsymbol{v}_1\cdot\nabla\phi_2 + \boldsymbol{v}_2\cdot\nabla\phi_1 + \epsilon\boldsymbol{v}_2\cdot\nabla\phi_2\right) \tag{2.25}$$

appearing on the right-hand side of (2.3) is a third-order contribution that can be neglected. Using (2.24) and (2.25) to evaluate (2.3), at second order we thus obtain

$$\frac{\partial}{\partial t}\left[\lambda A_e\phi - \sigma\nabla\cdot\left(\frac{A_e\nabla_\perp\phi}{B^2}\right)\right] = \nabla\cdot\left[A_e\left(\sigma\frac{\boldsymbol{B}\cdot\nabla\times\boldsymbol{v}_E}{B^2}-1\right)\boldsymbol{v}_E - \sigma A_e\frac{\boldsymbol{B}\times\nabla\boldsymbol{v}_E^2}{2B^2}\right]. \tag{2.26}$$

To check the consistency of the ordering assumptions leading to (2.26) we must verify that the ion fluid conservation laws are satisfied by the derived equation. First consider the total mass

$$M_V = m\int_V n\,\mathrm{d}V. \tag{2.27}$$

In this notation $V\subset\mathbb{R}^3$ is a bounded domain occupied by the plasma and $\mathrm{d}V$ the volume element in $\mathbb{R}^3$. The constancy of M follows immediately by noting that at leading order in ϕ

$$M_V = m\int_V A_e\left(1+\lambda\phi\right)\,\mathrm{d}V. \tag{2.28}$$

Then, using (2.26) and (2.23) we have

$$\frac{\mathrm{d}M_V}{\mathrm{d}t} = -m\int_{\partial V} A_e\boldsymbol{v}\cdot\boldsymbol{n}\,\mathrm{d}S, \tag{2.29}$$

where $\boldsymbol{n}$ is the unit outward normal to the boundary ∂V, $\mathrm{d}S$ is the surface element on ∂V and $\boldsymbol{v}$ is given by (2.23). This boundary integral vanishes if the system is periodic or the fluid velocity $\boldsymbol{v}$ is tangential to the bounding surface, $\boldsymbol{v}\cdot\boldsymbol{n}=0$ on ∂V, or $A_e=0$ on ∂V. Next, consider the fluid energy

$$E_V = \int_V n\left(\frac{1}{2}m\boldsymbol{v}^2 + Ze\phi\right)\,\mathrm{d}V. \tag{2.30}$$

To study conservation of energy it is convenient to subtract from E_V the total mass M_V and define a new quantity:

$$H_V = \frac{E_V}{Ze} - \frac{M_V}{m\lambda} = \int_V n\left(\frac{1}{2}\sigma\lambda\boldsymbol{v}^2 + \lambda\phi^2 - \frac{1}{\lambda}\right)\,\mathrm{d}V. \tag{2.31}$$

At leading order in ϕ we therefore obtain

$$H_V = \frac{1}{2}\int_V A_e\left(\sigma\boldsymbol{v}_E^2 + \lambda\phi^2 - \frac{2}{\lambda}\right)\,\mathrm{d}V. \tag{2.32}$$

https://doi.org/10.1017/S0022377822000514 Published online by Cambridge University Press

Since $A_e(\boldsymbol{x})$ is independent of time, the quantity H_V can be further simplified to

$$H_V = \frac{1}{2}\int_V A_e\left(\lambda\phi^2 + \sigma\frac{|\nabla_\perp\phi|^2}{B^2}\right)\mathrm{d}V. \tag{2.33}$$

Using (2.26), the rate of change in H_V is

$$\begin{aligned}
\frac{\mathrm{d}H_V}{\mathrm{d}t} &= \int_V A_e\left(\lambda\phi\phi_t + \frac{\sigma}{B^2}\nabla\phi\cdot\nabla_\perp\phi_t\right)\mathrm{d}V \\
&= \int_V \phi\left[\lambda A_e\phi_t - \sigma\nabla\cdot\left(\frac{A_e\nabla_\perp\phi_t}{B^2}\right)\right]\mathrm{d}V + \sigma\int_{\partial V} A_e\phi\frac{\nabla_\perp\phi_t}{B^2}\cdot\boldsymbol{n}\,\mathrm{d}S \\
&= \int_V \phi\nabla\cdot\left[A_e\left(\sigma\frac{\boldsymbol{B}\cdot\nabla\times\boldsymbol{v}_E}{B^2} - 1\right)\boldsymbol{v}_E - \sigma A_e\frac{\boldsymbol{B}\times\nabla\boldsymbol{v}_E^2}{2B^2}\right]\mathrm{d}V \\
&\quad + \sigma\int_{\partial V} A_e\phi\frac{\nabla_\perp\phi_t}{B^2}\cdot\boldsymbol{n}\,\mathrm{d}S \\
&= \int_{\partial V} A_e\phi\left[\left(\sigma\frac{\boldsymbol{B}\cdot\nabla\times\boldsymbol{v}_E}{B^2} - 1\right)\boldsymbol{v}_E - \sigma\frac{\boldsymbol{B}\times\nabla\boldsymbol{v}_E^2}{2B^2} + \sigma\frac{\nabla_\perp\phi_t}{B^2}\right]\cdot\boldsymbol{n}\,\mathrm{d}S \\
&\quad - \frac{1}{2}\sigma\int_V A_e\boldsymbol{v}_E\cdot\nabla\boldsymbol{v}_E^2\,\mathrm{d}V \\
&= -\int_{\partial V} A_e\phi\,\boldsymbol{v}\cdot\boldsymbol{n}\,\mathrm{d}S - \frac{1}{2}\sigma\int_V A_e\boldsymbol{v}_E\cdot\nabla\boldsymbol{v}_E^2\,\mathrm{d}V.
\end{aligned} \tag{2.34}$$

Here, $\boldsymbol{v}$ is given by (2.23) and the notation $\phi_t = \partial\phi/\partial t$ has been used. Notice that boundary integrals vanish if the system is periodic or $\boldsymbol{v}\cdot\boldsymbol{n} = 0$ on ∂V or $A_e\phi = 0$ on ∂V.

However, the last term on the right-hand side cannot be written as a boundary integral. Hence, an additional ordering condition is needed to ensure that energy is preserved. This term originates from the quantity

$$\sigma\nabla\cdot\left(A_e\frac{\boldsymbol{B}\times\nabla\boldsymbol{v}_E^2}{2B^2}\right) = \frac{1}{2}\sigma\nabla\boldsymbol{v}_E^2\cdot\nabla\times\left(\frac{A_e\boldsymbol{B}}{B^2}\right) \tag{2.35}$$

appearing on the right-hand side of (2.26). We therefore demand that

$$\frac{t_c\sigma}{2A_e}\left|\nabla\boldsymbol{v}_E^2\cdot\nabla\times\left(\frac{A_e\boldsymbol{B}}{B^2}\right)\right| \sim \epsilon^3. \tag{2.36}$$

Observe that the scaling above reflects the degree of accuracy of the ordering assumption $t_c^2L_\perp^{-1}\partial\boldsymbol{v}_2/\partial t \sim \epsilon$ adopted in (2.10*a*,*b*) which led to the omission of this term from fluid momentum balance. Recalling that $\boldsymbol{v}_E^2$ is second order in ϵ, if the density gradient is small $L_\perp|\nabla_\perp A_e|/A_e \sim \epsilon$ the condition (2.36) is automatically satisfied for those magnetic fields such that $B_0L_\perp\left|\nabla\times\left(B^{-2}\boldsymbol{B}\right)\right| \sim \epsilon$, with $B_0 \in \mathbb{R}$ a reference magnetic field, or equivalently

$$\boldsymbol{B} = B^2\left(\nabla\zeta + \epsilon\boldsymbol{\xi}\right) \tag{2.37}$$

for some potential ζ and vector field $\boldsymbol{\xi}$. This condition implies that the quantity $\boldsymbol{B}/B^2$ does not depart largely from a potential field, physically implying that the divergence of the $\boldsymbol{E}\times\boldsymbol{B}$ velocity scales as $t_c\nabla\cdot\boldsymbol{v}_E = t_c\epsilon\nabla\times\boldsymbol{\xi}\cdot\nabla\phi \sim \epsilon^2$. This is the case of the

https://doi.org/10.1017/S0022377822000514 Published online by Cambridge University Press

standard Hasegawa–Mima equation, where $L_\perp \left|\nabla_\perp A_e\right| / A_e \sim \epsilon$ and (2.36) is satisfied with $\zeta = B_0^{-1} z$, $B_0 \in \mathbb{R}$ and $\boldsymbol{\xi} = \mathbf{0}$ so that $\nabla \cdot \boldsymbol{v}_E = 0$. An alternative way to fulfil (2.36) is to assume that

$$L_\perp \left|\nabla \boldsymbol{v}_E^2\right| \sim \epsilon \boldsymbol{v}_E^2, \tag{2.38}$$

implying a mild change in $\boldsymbol{E} \times \boldsymbol{B}$ drift velocity across $\boldsymbol{B}$ as in the case for large-scale coherent structures studied in § 3.

Once the prescription (2.36) is enforced, the last term in (2.26) can be neglected since it scales as ϵ^3, and we obtain a consistent equation for the potential ϕ,

$$\frac{\partial}{\partial t}\left[\lambda A_e \phi - \sigma \nabla \cdot \left(\frac{A_e \nabla_\perp \phi}{B^2}\right)\right] = \nabla \cdot \left[A_e \left(\sigma \frac{\boldsymbol{B} \cdot \nabla \times \boldsymbol{v}_E}{B^2} - 1\right) \boldsymbol{v}_E\right], \tag{2.39}$$

which preserves the total mass (2.28) and the energy (2.33) exactly under suitable boundary conditions. In particular, one obtains

$$\frac{\mathrm{d}M_V}{\mathrm{d}t} = -m \int_{\partial V} A_e \boldsymbol{v}' \cdot \boldsymbol{n}\, \mathrm{d}S, \quad \frac{\mathrm{d}H_V}{\mathrm{d}t} = -\int_{\partial V} A_e \phi\, \boldsymbol{v}' \cdot \boldsymbol{n}\, \mathrm{d}S, \tag{2.40a,b}$$

with the effective ion fluid velocity

$$\boldsymbol{v}' = \left(1 - \sigma \frac{\boldsymbol{B} \cdot \nabla \times \boldsymbol{v}_E}{B^2}\right) \boldsymbol{v}_E - \sigma \frac{\partial}{\partial t} \frac{\nabla_\perp \phi}{B^2}. \tag{2.41}$$

The conditions on magnetic field topology for the existence of an additional conserved quantity (generalized enstrophy) are discussed in § 4.

We suggest that (2.39) is appropriate to describe electrostatic turbulence in magnetic fields with arbitrary topology. In particular, considering the ordering condition (2.36), the equation is best suited for magnetic fields of the type (2.37) so that $t_c \nabla \cdot \boldsymbol{v}_E \sim \epsilon^2$, or for configurations (2.38) such that the spatial change in $\boldsymbol{E} \times \boldsymbol{B}$ drift velocity scales as $t_c^2 L_\perp^{-1} \nabla \boldsymbol{v}_E^2 \sim \epsilon^3$.

It should be noted that (2.39) can be derived from the standard drift turbulence ordering $e\phi / k_B T_e \sim \Omega_c^{-1} \partial / \partial t \sim \epsilon$, $k_\perp L_\perp' \sim k_\perp L_{n_e} \sim k_\perp / k_\parallel \sim \epsilon^{-1}$ and $k_\perp \rho_s \sim 1$, where $L_\perp'$ is a large perpendicular scale associated with the spatial change in $\boldsymbol{B}$, $L_{n_e} \sim A_e / \left|\nabla_\perp A_e\right|$ the characteristic spatial scale associated with the density n_e, $k_\parallel$ a characteristic wavenumber along the magnetic field, $\rho_s = c_s m / ZeB$ the sound radius and $c_s = (Z k_B T_e / m)^{1/2}$ the sound speed. With such ordering the last term in (2.26) can be discarded from the outset, being a third-order contribution. However, this comes at the price of additional constraints on the spatial change allowed for $\boldsymbol{B}$, since all its spatial derivatives $L_\perp \nabla \sim 1 / k_\perp L_\perp' \sim \epsilon$ must be small.

Regarding the physical interpretation of the terms appearing in the equation, it is worth observing that the quantity $\nabla \cdot \left(B^{-2} \nabla_\perp \phi\right)$ arises from the component of the vorticity $\nabla \times \boldsymbol{v}_E$ along $\boldsymbol{B}$. Indeed,

$$\frac{\boldsymbol{B}}{B^2} \cdot \nabla \times \boldsymbol{v}_E = \nabla \cdot \left(\frac{\nabla_\perp \phi}{B^2}\right) + \left[\nabla \times \left(\frac{\boldsymbol{B}}{B^2}\right)\right] \times \frac{\boldsymbol{B}}{B^2} \cdot \nabla_\perp \phi. \tag{2.42}$$

In addition, a term $\nabla \cdot \left(n B^{-2} \nabla_\perp \phi\right)$ is often encountered in modern gyrokinetic and gyrofluid theories as the ion polarization charge density in Poisson's equation for the electric potential (Strinzi & Scott 2004; Hahm, Wang & Madsen 2009). The factor $1 - \sigma B^{-2} \boldsymbol{B} \cdot \nabla \times \boldsymbol{v}_E$ on the right-hand side of (2.39) is similarly predicted by gyrokinetic theory as a correction caused by the polarization charge-like term to the effective magnetic field strength:

$$B_{\parallel}^{*} \simeq B\left(1+\sigma\frac{\boldsymbol{B}\cdot\nabla\times\boldsymbol{v}_E}{B^2}\right), \tag{2.43}$$

which corresponds to the Jacobian determinant of the guiding centre phase space when parallel dynamics is ignored. This correction causes a net drift velocity (see equation (4) of Hahm (1996) or the discussion in Littlejohn (1981)):

$$\tilde{\boldsymbol{v}}_E = \frac{\boldsymbol{B}\times\nabla\phi}{BB_{\parallel}^{*}} \simeq \left(1-\sigma\frac{\boldsymbol{B}\cdot\nabla\times\boldsymbol{v}_E}{B^2}\right)\boldsymbol{v}_E. \tag{2.44}$$

3. Limit to the Hasegawa–Mima equation and curvature effects

In this section we show that (2.39) reduces to the Hasegawa–Mima equation (Hasegawa & Mima 1977*a*) when the magnetic field is straight, $\boldsymbol{B} = B_0\nabla z$ with $B_0 \in \mathbb{R}$. In the remainder of this paper, we restrict our attention to the constant density case $A_e \in \mathbb{R}$. In tokamak turbulence this condition can occur in the core of H-mode plasmas (Bernert *et al.* 2015) where density is often well approximated by a flat profile.

Before proceeding further, it should be noted that in many cases of practical interest the magnetic field varies on spatial scales $L_\perp$ that are larger than the sound radius ρ_s, i.e. $\rho_s/L_\perp \sim \epsilon$. If both magnetic field and electric potential vary on the macroscopic spatial scale $L_\perp$, the terms $\nabla\cdot(A_e\boldsymbol{v}_E)$ and $\nabla\cdot\left((\sigma/2)(A_e\boldsymbol{B}/B^2)\times\nabla\boldsymbol{v}_E^2\right)$ on the right-hand side of (2.26) become comparable third-order terms because

$$\frac{\nabla\cdot\left(\dfrac{\sigma}{2}\dfrac{A_e\boldsymbol{B}}{B^2}\times\nabla\boldsymbol{v}_E^2\right)}{\nabla\cdot(A_e\boldsymbol{v}_E)} = \frac{\dfrac{\sigma}{2}\nabla\boldsymbol{v}_E^2\cdot\nabla\times\left(\dfrac{A_e\boldsymbol{B}}{B^2}\right)}{\nabla\cdot(A_e\boldsymbol{v}_E)} \sim \epsilon^3\frac{\Omega_c}{v_E/L_\perp} \sim \epsilon^3\frac{\Omega_c eBL_\perp^2}{mc_s^2/Z}\frac{k_BT_e}{e\phi} \sim \epsilon^2\frac{L_\perp^2}{\rho_s^2}. \tag{3.1}$$

Hence, in this scenario the ordering breaks down. However, physical settings with $\rho_s/L_\perp \sim \epsilon$ can still be handled by invoking the standard Hasegawa–Mima ordering (which leads to the same (2.39) as previously explained) where the magnetic field changes on the large spatial scale $L_\perp$, while the electric potential is characterized by the smaller scale length ρ_s.

To elucidate how a curved inhomogeneous magnetic field modifies the Hasegawa–Mima equation, it is convenient to study (2.39) in the limit of a magnetic field of the type

$$\boldsymbol{B} = B_0\nabla z + \epsilon_B\boldsymbol{a}, \tag{3.2}$$

where $\epsilon_B \ll 1$ is an ordering parameter and $\boldsymbol{a} = \left(a_x, a_y, a_z\right)$ a vector field such that $\nabla\cdot\boldsymbol{a} = 0$. For simplicity, we assume that $a_z = \boldsymbol{a}\cdot\nabla z = 0$. Notice that the magnetic field (3.2) satisfies (2.37) and thus (2.36) as well. Furthermore, at the first order in ϵ_B the curvature of the magnetic field (3.2) is given by

$$\boldsymbol{\kappa} = \frac{\boldsymbol{B}}{B}\cdot\nabla\left(\frac{\boldsymbol{B}}{B}\right) = \frac{\epsilon_B}{B_0}\frac{\partial\boldsymbol{a}}{\partial z}. \tag{3.3}$$

It is convenient to introduce the two-dimensional gradient and Laplacian operators:

$$\nabla_{(x,y)}f = \frac{\partial f}{\partial x}\nabla x + \frac{\partial f}{\partial y}\nabla y, \quad \Delta_{(x,y)}f = \frac{\partial^2 f}{\partial x^2} + \frac{\partial^2 f}{\partial y^2}, \tag{3.4a,b}$$

https://doi.org/10.1017/S0022377822000514 Published online by Cambridge University Press

where $f = f(x, y, z)$ is some function. Then, at first order in ϵ_B we have

$$B^2 = B_0^2, \tag{3.5a}$$

$$\nabla_\perp \phi = \nabla_{(x,y)}\phi - \frac{\epsilon_B}{B_0}\left[(\boldsymbol{a}\cdot\nabla\phi)\,\nabla z + \frac{\partial\phi}{\partial z}\boldsymbol{a}\right], \tag{3.5b}$$

$$\boldsymbol{v}_E = \frac{\nabla z \times \nabla\phi}{B_0} + \frac{\epsilon_B}{B_0^2}\boldsymbol{a}\times\nabla\phi, \tag{3.5c}$$

$$\nabla\cdot\boldsymbol{v}_E = \frac{\epsilon_B}{B_0^2}\nabla\phi\cdot\nabla\times\boldsymbol{a}, \tag{3.5d}$$

$$\nabla\times\boldsymbol{v}_E = \frac{\Delta_{(x,y)}\phi}{B_0}\nabla z + \frac{\epsilon_B}{B_0^2}\nabla\times(\boldsymbol{a}\times\nabla\phi) - \frac{1}{B_0}\nabla_{(x,y)}\frac{\partial\phi}{\partial z}. \tag{3.5e}$$

Hence, defining the bracket

$$[f, g]_{(x,y)} = \frac{\partial f}{\partial x}\frac{\partial g}{\partial y} - \frac{\partial f}{\partial y}\frac{\partial g}{\partial x}, \tag{3.6}$$

with f, g some functions, (2.39) becomes

$$\begin{aligned}\frac{\partial}{\partial t}&\left[\lambda\phi - \frac{\sigma}{B_0^2}\Delta_{(x,y)}\phi + \frac{\epsilon_B\sigma}{B_0^3}\frac{\partial\boldsymbol{a}}{\partial z}\cdot\nabla\phi + \frac{2\epsilon_B\sigma}{B_0^3}\boldsymbol{a}\cdot\nabla\left(\frac{\partial\phi}{\partial z}\right)\right]\\ &= \frac{\sigma}{B_0^3}\left[\phi, \Delta_{(x,y)}\phi - \frac{2\epsilon_B}{B_0}\boldsymbol{a}\cdot\nabla\left(\frac{\partial\phi}{\partial z}\right)\right]_{(x,y)}\\ &\quad - \frac{\epsilon_B}{B_0^2}\left(1 - \frac{\sigma}{B_0^2}\Delta_{(x,y)}\phi\right)\nabla\phi\cdot\nabla\times\boldsymbol{a}\\ &\quad + \frac{\sigma\epsilon_B}{B_0^4}\nabla\phi\cdot\nabla\left(\Delta_{(x,y)}\phi\right)\times\boldsymbol{a}.\end{aligned} \tag{3.7}$$

Recalling (3.3), we see that the third term on the left-hand side of (3.7) arises from the curvature of the magnetic field. Terms involving $\partial\phi/\partial z$ describe the effect of the inhomogeneity of the electric potential along the vertical axis. The term including $\nabla\times\boldsymbol{B} = \epsilon_B\nabla\times\boldsymbol{a}$ can be ascribed to the presence of electric current in the system. Finally, the last term on the right-hand side results from the polarization drift associated with the component of the magnetic field $\epsilon_B\boldsymbol{a}$. Observe that (3.7) reduces to the Hasegawa–Mima equation when $\epsilon_B = 0$:

$$\frac{\partial}{\partial t}\left(\lambda\phi - \frac{\sigma}{B_0^2}\Delta_{(x,y)}\phi\right) = \frac{\sigma}{B_0^3}\left[\phi, \Delta_{(x,y)}\phi\right]_{(x,y)}. \tag{3.8}$$

The effect of the field curvature (3.3) can be made explicit by expanding $\boldsymbol{a}$ in Taylor series around $z = 0$, and by considering the dynamics on such a plane. At first order in z, one has

$$\boldsymbol{a} = \boldsymbol{a}_0 + z\boldsymbol{a}_1, \quad \boldsymbol{\kappa} = \frac{\epsilon_B}{B_0}\boldsymbol{a}_1, \tag{3.9a,b}$$

where $\boldsymbol{a}_0 = (a_{0x}, a_{0y}, 0)$ and $\boldsymbol{a}_1 = (a_{1x}, a_{1x}, 0)$ are vector fields independent of z. Using (3.9a,b) and setting $\partial\phi/\partial z = 0$, all terms in (3.7) lose the dependence on z, giving a

https://doi.org/10.1017/S0022377822000514 Published online by Cambridge University Press

two-dimensional equation:

$$\frac{\partial}{\partial t}\left(\lambda\phi - \frac{\sigma}{B_0^2}\Delta_{(x,y)}\phi + \frac{\sigma}{B_0^2}\boldsymbol{\kappa}\cdot\nabla\phi\right) = \frac{\sigma}{B_0^3}\left[\phi,\Delta_{(x,y)}\phi\right]_{(x,y)} - \frac{1}{B_0}\left(1 - \frac{\sigma}{B_0^2}\Delta_{(x,y)}\phi\right)\boldsymbol{\kappa}\times\nabla\phi\cdot\nabla z. \tag{3.10}$$

In many applications, the curvature of the magnetic field is not small. It is therefore instructive to examine how the Hasegawa–Mima equation is modified when curvature is a leading-order term. To this end, consider a circular magnetic field $\boldsymbol{B} = B_0 r\nabla\varphi$, where (r, φ, z) are cylindrical coordinates and $B_0 \in \mathbb{R}$. Notice that $\boldsymbol{B}^2 = B_0^2$ is constant (unlike the usual dependence $|\nabla\varphi|^2 = 1/r^2$), and that the curvature of the magnetic field is given by $\boldsymbol{\kappa} = -\nabla \log r$. Assuming that the condition (2.36), which in this case can be explicitly written as $r^{-1}\partial\,|\nabla_\perp\phi|^2/\partial z \sim \epsilon^3$, is initially satisfied by the electric potential ϕ, (2.39) can be written as

$$\frac{\partial}{\partial t}\left(\lambda\phi - \frac{\sigma}{B_0^2}\Delta_{(z,r)}\phi\right) = \frac{\kappa}{B_0}\frac{\partial\phi}{\partial z}\left(\frac{\sigma}{B_0^2}\Delta_{(z,r)}\phi - 1\right) - \frac{\sigma\kappa}{B_0^3}\left[\phi,\frac{\partial\phi}{\partial r}\right]_{(z,r)} + \frac{\sigma}{B_0^3}\left[\phi,\Delta_{(z,r)}\phi\right]_{(z,r)}, \tag{3.11}$$

where we introduced the differential operators

$$\nabla_{(z,r)}f = \frac{\partial f}{\partial z}\nabla z + \frac{\partial f}{\partial r}\nabla r,\quad \Delta_{(z,r)}f = \frac{1}{r}\frac{\partial}{\partial r}\left(r\frac{\partial f}{\partial r}\right) + \frac{\partial^2 f}{\partial z^2},\quad [f,g]_{(z,r)} = \frac{\partial f}{\partial z}\frac{\partial g}{\partial r} - \frac{\partial g}{\partial z}\frac{\partial f}{\partial r}. \tag{3.12a–c}$$

Notice that the field curvature modifies the Hasegawa–Mima equation through the modulus $\kappa^2 = 1/r^2$, and that (3.11) is two-dimensional if axial symmetry $\partial\phi/\partial\varphi = 0$ is assumed. Furthermore, since we expect the electric potential ϕ, the electric field $-\nabla_{(z,r)}\phi$ and the electric charge $-\Delta_{(z,r)}\phi$ to be bounded, the Hasegawa–Mima equation can be recovered in the limit $r\to\infty$ ($\kappa\to 0$) where field lines become progressively straight. Next, observe that in the Hasegawa–Mima equation (3.8) steady states are given by the equation $[\phi, \Delta_{(x,y)}\phi] = 0$, or simply $\Delta_{(x,y)}\phi = -f(\phi)$ with f some function of ϕ. Since the electric charge $-\Delta_{(x,y)}\phi$ should vanish when $\phi = 0$, for small ϕ we may set $f = f_0\phi$ with f_0 a positive real constant (the positive sign physically means that charge density gradients $-\nabla_{(x,y)}\Delta_{(x,y)}\phi$ are directed in the opposite direction to the electric field $-\nabla_{(x,y)}\phi$). Then, considering a two-dimensional domain $(x, y) \in V = [0, \pi]^2$ such that the electric potential is grounded on the boundary, i.e. $\phi = 0$ on ∂V, solution of the steady Hasegawa–Mima equation gives self-organized states of the type $\phi = \phi_0 \sin(mx)\sin(ny)$ with $\phi_0 \in \mathbb{R}$, $m, n \in \mathbb{Z}$ and $f_0 = m^2 + n^2$. Since f_0 corresponds to the ratio between enstrophy and energy in the fluid limit $\lambda = 0$, at equilibrium the minimum possible value $f_0 = 2$ corresponding to $m = n = 1$ is expected to be preferentially selected (see e.g. Hasegawa (2004) on this point). Let us see how the situation changes in a curved magnetic field. Since the right-hand side of (3.11) can be written as

$$\frac{1}{r}\left[\phi, -\frac{r}{B_0} - \frac{\sigma}{B_0^3}\frac{\partial\phi}{\partial r} + \frac{\sigma}{B_0^3}r\Delta_{(z,r)}\phi\right]_{(z,r)}, \tag{3.13}$$

steady states in the circular magnetic field $\boldsymbol{B} = B_0 r\nabla\phi$ are described by the equation

$$\frac{\sigma}{B_0^3}\left(\frac{\partial^2\phi}{\partial r^2} + \frac{\partial^2\phi}{\partial z^2}\right) = \frac{1}{B_0} - \frac{f(\phi)}{r}. \tag{3.14}$$

https://doi.org/10.1017/S0022377822000514 Published online by Cambridge University Press

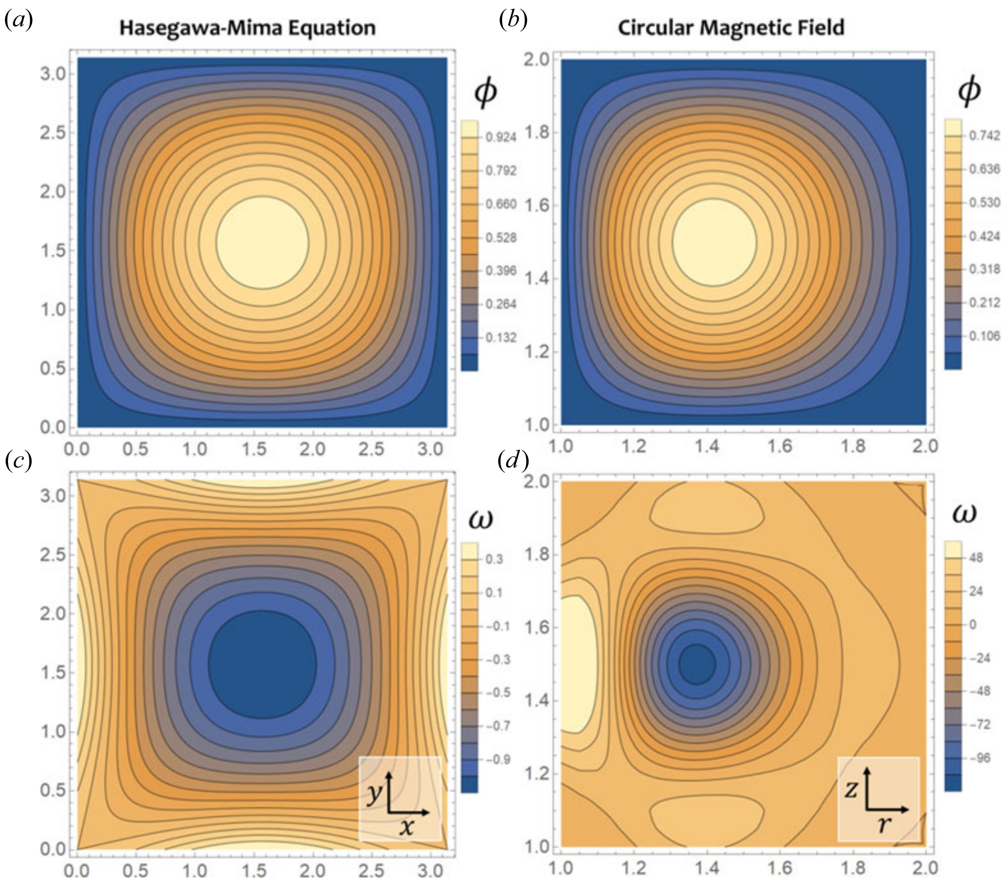

FIGURE 1. (a,b) Contour plots of the self-organized steady electric potential ϕ in a straight magnetic field $\boldsymbol{B} = B_0 \nabla z$ (Hasegawa–Mima equation) and in a circular magnetic field $\boldsymbol{B} = B_0 r \nabla \varphi$. ($c$,$d$) Contour plots of the respective vorticities $\omega = \nabla \times \boldsymbol{v} \cdot \nabla z$ and $\omega = \nabla \times \boldsymbol{v} \cdot r\nabla\varphi$ with the ion fluid velocity $\boldsymbol{v}$ defined by (2.41). In this simulation, $B_0 = 1$ and $f_0 = 2$ for the Hasegawa–Mima case, while $B_0 = 1$, $\sigma = 0.1$ and $f_0 = 1$ for the circular magnetic field case.

Considering the case $f = f_0\phi$ and taking a two-dimensional toroidal domain with squared cross-section $(r, z) \in V = [1, 2]^2$ and Dirichlet boundary conditions $\phi = 0$ on the boundary ∂V, solution of (3.14) results in a self-organized steady state sustained by the curvature of the magnetic field. Figure 1 shows contour plots of the steady electric potential ϕ and vorticity $\omega = \nabla \times \boldsymbol{v} \cdot r\nabla\varphi$ with $\boldsymbol{v}$ given by (2.41) obtained by numerical solution of (3.14) as compared with the Hasegawa–Mima case. The corresponding fluid drifts $\boldsymbol{v}_E$ and $\boldsymbol{v}$ are given in figure 2. From these figures, one sees that contours of electric potential ϕ, vorticity ω and fluid drifts $|\boldsymbol{v}_E|$ and $|\boldsymbol{v}|$ tend to accumulate in regions of higher curvature (small radius r), implying the onset of steeper gradients, while inhomogeneities are suppressed where the curvature is weaker. Figure 2 also reveals that the fluid drifts $\boldsymbol{v}_E$ and $\boldsymbol{v}$ are enhanced where the curvature is stronger. We remark that the observed behaviour is not caused by the gradient or curvature drifts of the guiding centre framework because the cold ions approximation is being considered. In addition, the background magnetic field has uniform strength in this example. Hence, curvature affects self-organized states through the $\boldsymbol{E} \times \boldsymbol{B}$ drift, as clear from (2.39).

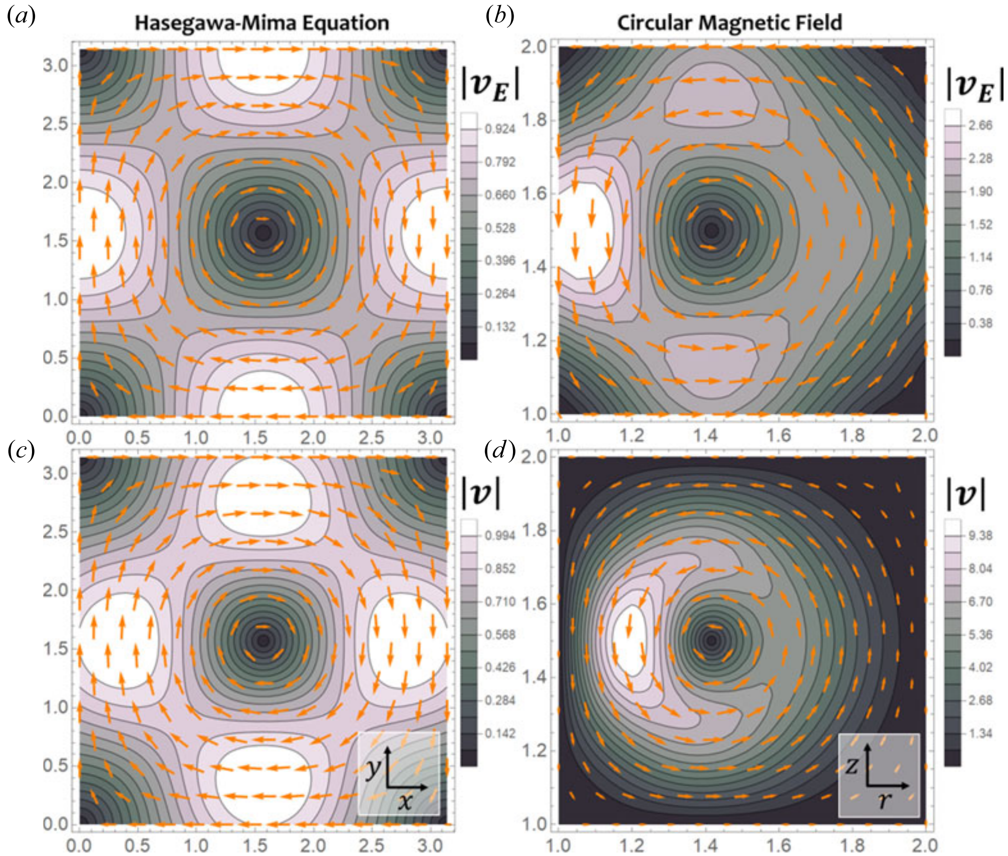

FIGURE 2. (*a*,*b*) Vector plots of the $\boldsymbol{E} \times \boldsymbol{B}$ drift velocity $\boldsymbol{v}_E$ associated with the steady states of figure 1 and contour plots of the modulus $|\boldsymbol{v}_E|$. (*c*,*d*) Vector plots of the corresponding total ion fluid velocity $\boldsymbol{v}$ of (2.41) and contour plots of the modulus $|\boldsymbol{v}|$.

The effect of vertical inhomogeneity in the potential ϕ can be further examined by setting $\phi = q + \sin(mz)\, p$, with $q(r)$ and $p(r)$ radial functions and $m \in \mathbb{Z}$. Then, (3.14) reduces to the system

$$\frac{\sigma}{B_0^3}\frac{\partial^2 p}{\partial r^2} + \left(\frac{f_0}{r} - m^2\frac{\sigma}{B_0^3}\right)p = 0, \quad \frac{\sigma}{B_0^3}\frac{\partial^2 q}{\partial r^2} + \frac{f_0}{r}q - \frac{1}{B_0} = 0. \tag{3.15a,b}$$

A plot of the electric potential ϕ obtained by solution of system (3.15*a*,*b*) for different values of m and B_0 is given in figure 3. Notice that for a sufficiently large magnetic field strength B_0, structures arise in the radial direction as well. The size and spacing of these radial structures appear to be modulated by the background strength and curvature of the magnetic field rather than the constant m associated with the vertical oscillation.

4. The case of curved magnetic fields crossing a surface perpendicularly

The Hasegawa–Mima equation is endowed with two inviscid invariants, the total energy and the generalized enstrophy. The generalized enstrophy is an invariant arising from the two-dimensional nature of the governing equation, which is restricted to the flat (x, y) plane with normal given by the straight vertical magnetic field $\boldsymbol{B} = B_0\nabla z$. It is useful

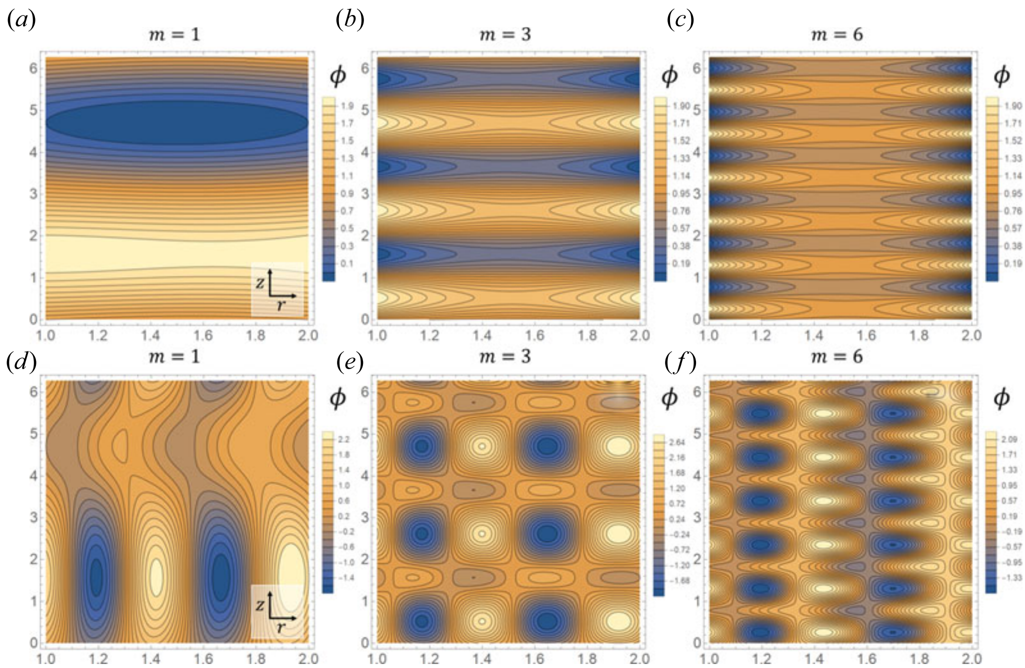

FIGURE 3. Contour plots of the electric potential ϕ obtained by solution of (3.15*a*,*b*) for different values of m and B_0. Dirichlet boundary conditions $p(1) = p(2) = 1$ and $q(1) = q(2) = 1$ are used. The case $m = 1$ for (*a*) $B_0 = 1$ and (*d*) $B_0 = 5$. The case $m = 3$ for (*b*) $B_0 = 1$ and (*e*) $B_0 = 5$. The case $m = 6$ for (*c*) $B_0 = 1$ and (*f*) $B_0 = 5$. In this simulation $\sigma = 0.5$ and $f_0 = 1$.

to consider the conditions under which the same kind of topological invariant persists in general magnetic fields. A condition for the analogy with two-dimensional vorticity dynamics to apply is that the magnetic field defines the normal direction of a general (not necessarily flat) two-dimensional surface $\Sigma \subset \mathbb{R}^3$. In this case, the dynamics is restricted to the surface Σ because the drift velocity (2.23) satisfies $\boldsymbol{B} \cdot \boldsymbol{v} = 0$. The geometric condition for a vector field $\boldsymbol{B}$ to locally define the normal of a surface Σ is given by the Frobenius integrability condition (Frankel 2012):

$$\boldsymbol{B} \cdot \nabla \times \boldsymbol{B} = 0. \tag{4.1}$$

In particular, if the magnetic field $\boldsymbol{B}$ has vanishing helicity density then there exist locally defined functions α, C such that

$$\boldsymbol{B} = \alpha \nabla C. \tag{4.2}$$

The magnetic field $\boldsymbol{B}$ thus defines the normal to the surface $C =$ constant. When $\alpha = \alpha(C)$, the magnetic field $\boldsymbol{B}$ becomes a vacuum magnetic field because $\nabla \times \boldsymbol{B} = \boldsymbol{0}$. In this section, we are concerned with magnetic fields of the type (4.2). We will assume that the functions α and C exist in the domain V, and that $\boldsymbol{B} \neq \boldsymbol{0}$ in V. It is worth noticing that for time-independent magnetic fields the constraint (4.1) corresponds to the requirement that the electric current $\boldsymbol{J} = \nabla \times \boldsymbol{B}$ is always perpendicular to the magnetic field, $\boldsymbol{J} \cdot \boldsymbol{B} = 0$. In tokamaks this condition will be rarely satisfied because most of the plasma current is aligned with the magnetic field. In addition, we remark that adiabatic electron response underlying the generalized Hasegawa–Mima equation (2.39) may impose additional constraints on the magnetic field configuration. Indeed, one expects

https://doi.org/10.1017/S0022377822000514 Published online by Cambridge University Press

adiabatic electron response to hold only when the integral curves of the magnetic field form closed surfaces, with generally non-rational rotational transform.

Next, recall that the magnetic field $\boldsymbol{B}$ must be solenoidal. Hence, the Lie–Darboux theorem (Arnold 1989; de Léon 1989) applies: locally there exist functions Ψ, θ such that

$$\boldsymbol{B} = \nabla\Psi \times \nabla\theta. \tag{4.3}$$

Again, we will assume that the functions Ψ and θ are well defined in the domain V. A typical example of vacuum magnetic field is the magnetic field generated by a point dipole. In this case

$$\alpha = 1, \quad C = -M\frac{z}{\left(r^2+z^2\right)^{3/2}}, \quad \Psi = M\frac{r^2}{\left(r^2+z^2\right)^{3/2}}, \quad \theta = \varphi, \tag{4.4a–d}$$

where (r, φ, z) are cylindrical coordinates and M a physical constant with units of $\mathrm{T\,m^3}$. The functions (C, Ψ, θ) can be used as a system of curvilinear coordinates. The Jacobian determinant of the coordinate transformation is given by

$$J = \nabla C \cdot \nabla\Psi \times \nabla\theta = \frac{B^2}{\alpha}. \tag{4.5}$$

Given two functions f, g it is convenient to introduce the bracket

$$\left[f, g\right]_{(\Psi,\theta)} = \frac{\partial f}{\partial\Psi}\frac{\partial g}{\partial\theta} - \frac{\partial f}{\partial\theta}\frac{\partial g}{\partial\Psi}. \tag{4.6}$$

Using (4.6), the derived (2.39) can be written as

$$\frac{\partial}{\partial t}\left[\lambda\phi - \sigma\nabla\cdot\left(\frac{\nabla_\perp\phi}{B^2}\right)\right] = \frac{B^2}{\alpha}\left[\phi, -\frac{\alpha}{B^2} + \sigma\frac{\alpha^2}{B^4}\nabla\cdot\left(\frac{\nabla_\perp\phi}{\alpha}\right)\right]_{(\Psi,\theta)}. \tag{4.7}$$

One can verify that under appropriate boundary conditions on the surface boundary $\partial\Sigma$ the surface energy

$$H_\Sigma = \frac{1}{2}\int_\Sigma\left(\lambda\phi^2 + \sigma\frac{|\nabla_\perp\phi|^2}{B^2}\right)\frac{\alpha}{B^2}\,\mathrm{d}\Psi\,\mathrm{d}\theta \tag{4.8}$$

is a constant of (4.7). The condition for conservation of generalized enstrophy,

$$W_\Sigma = \frac{1}{2}\int_\Sigma\left\{\lambda\frac{|\nabla_\perp\phi|^2}{B^2} + \sigma\left[\nabla\cdot\left(\frac{\nabla_\perp\phi}{B^2}\right)\right]^2\right\}\frac{\alpha}{B^2}\,\mathrm{d}\Psi\,\mathrm{d}\theta, \tag{4.9}$$

can be obtained by noting that the second argument of the bracket on the right-hand side of (4.7) must be a function of $\nabla\cdot\left(B^{-2}\nabla_\perp\phi\right)$ up to a function of ϕ. The condition is

$$\alpha = \frac{k}{|\nabla C|^2} = \frac{B^2}{k}, \quad k\in\mathbb{R}, \tag{4.10}$$

which is equivalent to

$$\nabla\times\left(\frac{\boldsymbol{B}}{B^2}\right) = \boldsymbol{0}. \tag{4.11}$$

https://doi.org/10.1017/S0022377822000514 Published online by Cambridge University Press

In this case, $\nabla \cdot \boldsymbol{v}_E = \nabla\phi \cdot \nabla \times \left(B^{-2}\boldsymbol{B}\right) = 0$. Notice also that $\nabla \cdot \boldsymbol{B} = 0$ implies that configurations of the type (4.10) must satisfy

$$\nabla \cdot \left(\frac{\nabla C}{|\nabla C|^2}\right) = 0. \tag{4.12}$$

In spherical geometry, denoting with R the spherical radius, a magnetic field satisfying (4.10) and (4.12) can be obtained by setting

$$\alpha = \frac{B_0}{R^4}, \quad B_0 \in \mathbb{R}, \quad C = \frac{R^3}{3}. \tag{4.13a–c}$$

Similarly, in cylindrical geometry, magnetic fields compatible with (4.10) and (4.12) include those generated by

$$\alpha = \frac{B_0}{r^2}, \quad B_0 \in \mathbb{R}, \quad C = \frac{r^2}{2}, \tag{4.14a}$$

$$\alpha = B_0 r^2, \quad B_0 \in \mathbb{R}, \quad C = \varphi. \tag{4.14b}$$

Observe that when $\lambda = 0$ (4.7) with either (4.13*a–c*) or (4.14a) gives the usual two-dimensional vorticity dynamics on a sphere or cylinder respectively. The case of (4.14b) corresponds to a circular magnetic field $\boldsymbol{B} = B_0 r^2 \nabla\varphi$ with curvature $\boldsymbol{\kappa} = -\nabla \log r$. Assuming axial symmetry $\phi = \phi(r, z)$, the corresponding form of (2.39) is again two-dimensional:

$$\frac{\partial}{\partial t}\left[\lambda\phi - \frac{\sigma}{B_0^2}\nabla \cdot \left(\kappa^2 \nabla_{(z,r)}\phi\right)\right] = \frac{\sigma}{B_0^3}\kappa \left[\phi, \nabla \cdot \left(\kappa^2 \nabla_{(z,r)}\phi\right)\right]_{(z,r)}. \tag{4.15}$$

5. Concluding remarks

In conclusion, we have derived a model equation (2.39) describing electrostatic plasma turbulence in a general magnetic field. The equation preserves the mass (2.28) and the energy (2.33), and reduces to the Hasegawa–Mima equation in the limit of a straight magnetic field. The ordering adopted in the derivation of the equation is slightly different from the classical one. On the one hand, both the magnetic field and the electrostatic potential are allowed to vary on the same spatial scale. On the other hand, the requirement (2.36), which is automatically satisfied in the standard setting of the Hasegawa–Mima equation, ensures the consistency of the ordering with respect to preservation of energy. This latter condition implies that the derived equation is best suited for magnetic fields satisfying (2.37), implying a second-order $\boldsymbol{E} \times \boldsymbol{B}$ drift velocity divergence, or for spatial scales such that the change in $\boldsymbol{v}_E^2$ represents a third-order contribution (2.38). Nevertheless, as discussed at the end of § 2 the same (2.39) can be obtained from the standard ordering, at the price of more stringent constraints on the spatial behaviour of the magnetic field.

Conservation of generalized enstrophy holds when the magnetic field defines the normal of a surface and it is compatible with two-dimensional vorticity dynamics. It should be noted that inverse energy cascades are expected to occur for all magnetic configurations such that generalized enstrophy is constant. Indeed, the order of ϕ derivatives appearing in (4.8) and (4.9) is not changed by the geometry of the background magnetic field. Detailed analysis of the effect of magnetic topology on inverse cascades and zonal flows is left for future work.

As a physical application of the obtained equation, we have studied how the curvature of a circular magnetic field with uniform strength modifies self-organized steady states by comparison with analogous equilibria in a straight magnetic field. A strong curvature tends to attract level sets of electric potential and vorticity, and to enhance fluid drift velocity. A higher curvature also appears to contribute to higher heterogeneity in the electric potential. This behaviour cannot be ascribed to gradient and curvature drifts occurring in the guiding centre picture because the model relies on the cold ions approximation. Hence, the effect of curvature is mediated by the $\boldsymbol{E} \times \boldsymbol{B}$ drift.

Finally, the results reported in this paper may be useful for constructing simplified models of turbulence in complex plasma systems of practical interest. In particular, we expect the derived equation to serve as a toy model of turbulence in tokamak and stellarator plasmas.

Acknowledgements

The authors are grateful to anonymous referees whose comments and suggestions greatly improved the paper.

Editor Per Helander thanks the referees for their advice in evaluating this article.

Funding

This work was partially supported by JSPS KAKENHI (N.S., grant nos. 21K13851, 17H01177).

Declaration of interests

The authors report no conflict of interest.

REFERENCES

ARNOLD, V.I. 1989 A symplectic atlas. In *Mathematical Methods of Classical Mechanics*, pp. 230–232. Springer.

BATCHELOR, G.K. 1969 Computation of the energy spectrum in homogeneous two-dimensional turbulence. *The Physics of Fluids Vol*. **12** (II), 233–239.

BERNERT, M., EICH, T., KALLENBACH, A., CARRALERO, D., HUBER, A., LANG, P.T., POTZEL, S., REIMOLD, F., SCHWEINZER, J., VIEZZER, E. *et al.* 2015 The h-mode density limit in the full tungsten asdex upgrade tokamak. *Plasma Phys. Control. Fusion* **57**, 1–12.

BRIZARD, A.J. & HAHM, T.S. 2007 Foundations of nonlinear gyrokinetic theory. *Rev. Mod. Phys*. **79**, 421–468.

CARY, J.R. & BRIZARD, A.J. 2009 Hamiltonian theory of guiding-center motion. *Rev. Mod. Phys. Vol.* **81** (2), 693–738.

CHARNEY, J.G. 1948 On the scale of atmospheric motions. *Geof. Publ. Vol*. **17** (2), 3–17.

CHARNEY, J.G. & DRAZIN, P.G. 1961 Propagation of planetary-scale disturbances from the lower into the upper atmosphere. *J. Geophys. Res. Vol*. **66** (1), 83–109.

DIAMOND, P.H., HASEGAWA, A. & MIMA, K. 2011 Vorticity dynamics, drift wave turbulence, and zonal flows: a look back and a look ahead. *Plasma Phys. Control. Fusion* **53**, 124001.

DRITSCHEL, D.G., QI, W. & MARSTON, J.B. 2015 On the late-time behavior of a bounded, inviscid two-dimensional flow. *J. Fluid Mech*. **783**, 1–22.

DUBIN, D.H.E., KROMMES, J.A. & OBERMAN, C. 1983 Nonlinear gyrokinetic equations. *The Physics of Fluids* **26**, 3524–3535.

FRANKEL, T. 2012 Holonomic and nonholonomic constraints. In *The Geometry of Physics*, pp. 165–171. Cambridge University Press.

FUJISAWA, A., ITOH, K., IGUCHI, H., MATSUOKA, K., OKAMURA, S., SHIMIZU, A., MINAMI, T., YOSHIMURA, Y., NAGAOKA, K., TAKAHASHI, C. *et al.* 2004 Identification of zonal flows in a toroidal plasma. *Phys. Rev. Lett*. **93**, 165002.

HAHM, T.S. 1996 Nonlinear gyrokinetic equations for turbulence in core transport barriers. *Phys. Plasmas* **3**, 4658–4664.

HAHM, T.S. & TANG, W.M. 1996 Nonlinear theory of collisionless trapped ion modes. *Phys. Plasmas* **3**, 242–247.

HAHM, T.S., WANG, L. & MADSEN, J. 2009 Fully electromagnetic nonlinear gyrokinetic equations for tokamak edge turbulence. *Phys. Plasmas* **16**, 022305.

HASEGAWA, A. 2004 Self-organization processes in continuous media. *Adv. Physics Vol.* **34** (1), 1–42.

HASEGAWA, A. & MIMA, K. 1977*a* Pseudo-three-dimensional turbulence in magnetized nonuniform plasma. *Phys. Fluids Vol.* **21** (1), 87–92.

HASEGAWA, A. & MIMA, K. 1977*b* Stationary spectrum of strong turbulence in magnetized nonuniform plasma. *Phys. Rev. Lett. Vol.* **39** (4), 205–208.

HASEGAWA, A. & MIMA, K. 2018 Strong turbulence, self-organization and plasma confinement. *Eur. Phys. J. H* **43**, 499–521.

HASEGAWA, A. & WAKATANI, M. 1983 Plasma edge turbulence. *Phys. Rev. Lett. Vol.* **50** (9), 682–686.

HASEGAWA, A. & WAKATANI, M. 1987 Self-organization of electrostatic turbulence in a cylibdrical plasma. *Phys. Rev. Lett. Vol.* **59** (14), 1581–1584.

HAZELTINE, R.D. 1983 Reduced magnetohydrodynamics and the Hasegawa–Mima equation. *Phys. Fluids Vol.* **26** (11), 3242–3245.

HAZELTINE, R.D., HSU, C.T. & MORRISON, P.J. 1987 Hamiltonian four-field model for nonlinear tokamak dynamics. *The Physics of Fluids Vol.* **30** (10), 3204–3211.

HAZELTINE, R.D. & WAELBROECK, F.L. 1998 In *The Framework of Plasma Physics*, pp. 67, 31. Perseus Books.

HORTON, W. 1999 Drift waves and transport. *Rev. Mod. Phys. Vol.* **71** (3), 735–778.

HORTON, W. & HASEGAWA, A. 1994 Quasi-two-dimensional dynamics of plasmas and fluids. *Chaos Vol.* **4** (2), 227–251.

KAUFMAN, A.N. 1986 The electric dipole of a guiding center and the plasma momentum density. *The Physics of Fluids Vol.* **29** (5), 1736–1737.

KRAICHNAN, R.H. 1967 Inertial ranges in two-dimensional turbulence. *The Physics of Fluids Vol.* **10** (7), 1417–1423.

KRAICHNAN, R.H. & MONTGOMERY, D. 1980 Two-dimensional turbulence. *Rep. Prog. Phys.* **43**, 547–619.

KROMMES, J.A. 2002 Fundamental statistical descriptions of plasma turbulence in magnetic fields. *Phys. Rep.* **360**, 1–352.

DE LÉON, M. 1989 Symplectic manifolds and cotangent bundles. In *Methods of Differential Geometry in Analytical Mechanics*, pp. 250–253. Elsevier.

LITTLEJOHN, R.G. 1981 Hamiltonian formulation of guiding center motion. *The Physics of Fluids* **24**, 1730–1749.

MORRISON, P.J. 1998 Hamiltonian description of the ideal fluid. *Rev. Mod. Phys.* **70**, 467–521.

NAZARENKO, S. & QUINN, B. 2009 Triple cascade behavior in quasigeostrophic and drift turbulence and generation of zonal jets. *Phys. Rev. Lett.* **103**, 118501.

NUMATA, R., BALL, R. & DEWAR, R.L. 2007 Bifurcation in electrostatic resistive drift wave turbulence. *Phys. Plasmas* **14**, 102312.

OBUSE, K., TAKEHIRO, S. & YAMADA, M. 2010 Long-time asymptotic states of forced two-dimensional barotropic incompressible flows on a rotating sphere. *Physics of Fluids* **22**, 056601.

RIVERA, M.K., DANIEL, W.B., CHEN, S.Y. & ECKE, R.E. 2003 Energy and enstrophy transfer in decaying two-dimensional turbulence. *Phys. Rev. Lett. Vol.* **90** (10), 1–4.

SINGH, R. & DIAMOND, P.H. 2021 A unified theory of zonal flow shears and density corrugations in drift wave turbulence. *Plasma Phys. Control. Fusion* **63**, 035015.

STRINZI, D. & SCOTT, B. 2004 Nonlocal nonlinear electrostatic gyrofluid equations. *Phys. Plasmas* **11**, 5452–5461.

TASSI, E., CHANDRE, C. & MORRISON, P.J. 2009 Hamiltonian derivation of the Charney–Hasegawa–Mima equation. *Phys. Plasmas* **16**, 082301.

WAKATANI, M. & HASEGAWA, A. 1984 A collisional drift wave description of plasma edge turbulence. *The Physics of Fluids Vol.* **27** (611), 611–618.

WEINSTEIN, A. 1983 Hamiltonian structure for drift waves and geostrophic flow. *The Physics of Fluids* **26**, 388–390.

XIAO, Z., WAN, M., CHEN, S. & EYINK, G.L. 2009 Physical mechanism of the inverse energy cascade of two-dimensional turbulence: a numerical investigation. *J. Fluid Mech.* **619**, 1–44.

YODEN, S. & YAMADA, M. 1993 A numerical experiment on two-dimensional decaying turbulence on a rotating sphere. *J. Atmos. Sci.* **50**, 631–644.